VIETNAM JOURNAL OF HYDROMETEOROLOGY

Research Article

An alternative calibration method for wave-fence interaction in SWASH model

Hoang Tung Dao[1*], Tri Mai[2], Cong Mai[3,4], Tuan Minh Thanh Doan[5]

[1] Hanoi University of Natural Resources and Environment, Vietnam; dhtung@hunre.edu.vn
[2] Hanoi University of Civil Engineering, Vietnam; trimc@nuce.edu.vn
[3] Thuyloi University, Vietnam; cong.m.v@tlu.edu.vn
[4] Delft University of Technology, the Netherlands; C.MaiVan@tudelft.nl;
[5] Ministry of Agriculture and Rural Development, Vietnam; minhthanhbql@gmail.com

*Corresponding author: dhtung@hunre.edu.vn; Tel.: +84–395357993

Received: 8 July 2022; Accepted: 19 August 2022; Published: 25 September 2022

Abstract: The application of brushwood fences along the Mekong deltaic coast has recently played a significant role in wave damping and promoting sedimentation. The insight mechanism of brushwood fence for wave energy reduction is the bulk drag coefficient ($\overline{C_D}$) that is also linked to the well-known Forchheimer coefficients (α, β). The bulk drag coefficient was then applied in the SWASH model for validation in its implementation model, the vegetation model, and showed a good comparison with the physical model in the same settings. The porosity model in the SWASH model applied the Forchheimer coefficient has not been used for validation even though the strong links between the $\overline{C_D}$ and the α, β were indicated. In this study, the validation of wave-fence interaction in the porosity model of the SWASH model is presented and compared to the vegetation model in the previous study. The results show a good agreement of wave heights and wave spectrum between the physical, vegetation and porosity models. Furthermore, the computational and physical model errors, such as BIAS and SI values, are less than 1 mm and 10%, respectively.

Keywords: Wooden fence; SWASH model; Mekong Delta; Darcy-Forchheimer.

1. Introduction

Coastal structures, such as breakwater, sea dikes, porous breakwater and wooden fences, bring a certain level of safety to marine habitats and people living along the coasts. However, the safe level of structures certainly depends on each type of structure applied [1]. For example, hard or grey structures, breakwater, and sea dikes create an acceleration of sediment transport at the upstream flow. In contrast, erosion apparently occurs on the downstream side of the structures due to breaking sediment equilibrium. On the other hand, porous structures or hybrid structures, such as either submerged or emerging structures, may reduce and occasionally stop the erosion at the downstream site. In the better case, a nature-based solution that combines a porous structure and a natural ecosystem can create a good situation for both inhabitants and natural vegetation, such as mangroves, along the coast.

The Mekong deltaic coastline has been under serve erosion conditions for more than a decade. The consequence of eroding the coastal zone brings many negative impacts to the living habitats along the coast. For example, natural marine ecosystems, mangroves, are now

facing a dangerous situation when the reduction of mangroves belt to the shore has been up to 50 to 100 m per year [2]. Furthermore, erosion phenomenon occurs along the coast can threaten the economic stability and the safety of civilization.

Along the Mekong deltaic coast, wooden fences are built in front of mangrove belts to reduce wave and flow energies and to increase the sedimentation inside the downstream basin. Furthermore, wooden fence structures with a maximum of three rows of vertical bamboo poles form a frame to keep horizontal brushwood, such as bamboo and tree branches [3–5]. The results of about 80% incoming wave height reduction were recorded at Nha Mat, Bac Lieu [3–6] and simulated in numerical studies [7–9]. However, due to a lack of understanding of flow over wooden fences, the study [10] carried out flow resistance experiments to indicate the bulk drag coefficient ($\overline{C_D}$) and the Forchheimer coefficients (α, β) of the wooden fences. Thereafter, the study [9] used the bulk drag coefficient for validating the wave-fence interaction data from the physical model with the simulated data in the SWASH model, developed by Delft University of Technology [9].

In the SWASH model, the vegetation implementation model simulates the interaction of waves and cylinders based on the well-known bulk drag coefficient. This coefficient can be indicated by the relationship between flow patterns and the array of cylinders [11–12], which is also influenced by the characteristic of cylinders themselves, for example, the cylinder surface, the cylinder diameters, and positions between cylinders [13–14]. On the other hand, the porous implementation model considers the famous Forchheimer coefficients from the Darcy-Forchheimer equations to indicate the drag forces [15–16] if the array of cylinders can be considered as permeable media. Therefore, the drag forces on porous media were then indicated as the linear and nonlinear forces caused by the effect of laminar and turbulent friction, respectively [17–18].

In the previous study [9], well agreements between physical and numerical models were presented, which applied the bulk drag coefficient found in the study [10]. However, the interesting simulation for the porous implementation model has been abandoned. Therefore, in this study, this simulation of the porous model is presented that validates the measurement data and the numerical modelling of the vegetation model [9].

2. Method

2.1. Physical model

The physical model of wave-fence interactions was conducted in the wave flume at the Hydraulic Engineering Laboratory at Delft University of Technology. The settings of wave piston, wave gauges and wooden fences are shown in Figure 1.

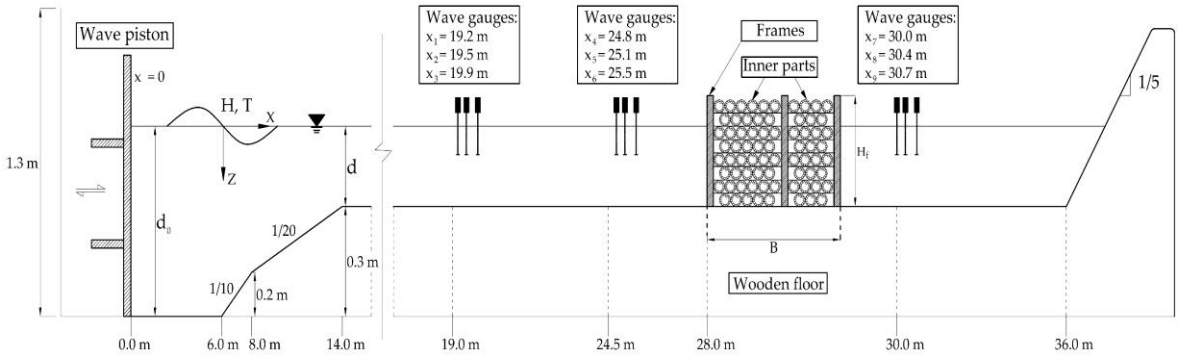

Figure 1. The cross profile is used in physical and numerical models [9].

The wave conditions were put on the west side of the flume, while a schematized dike was located on the east side. The horizontal bed is to schematize the gentle foreshore along the Mekong deltaic coast, creating a breaking zone for waves. However, the flume in the

laboratory was virtually short and made an impossible design for a gentle slope. Therefore, steep slopes were combined to simulate similar breaking phenomena. Furthermore, waves were intended to break at x = 14.0 m before reaching the fence at x = 28.0 m on the horizontal bed (Figure 1).

Wave conditions were used in physical and numerical models, including irregular wave heights (H_s) and peak wave periods (T_P) ranged from 0.035 to 0.075 m and from 1.1 to 2.7 seconds, respectively. Three water depths (d) were used as 0.15, 0.20, and 0.25 m corresponding to three fence thicknesses. The settings for wooden fences were inhomogeneous with bamboo cylinders with diameters of about 0.004 m. The setup and structures are shown in Figure 2. Wooden fences used in this physical model had three different thicknesses, B = 0.28, 0.40, and 0.66 m, while the height was fixed at 0.30 m. In every test, the number of cylinders in m^2 was also fixed at 8705 cylinder/m^2 resulting in a density of 0.10 or porosity of 0.90. Moreover, wave data were recorded by a total of nine wave gauges (WGs) from WG1 to WG9 (Figure 1) with a sampling frequency of 100 H.

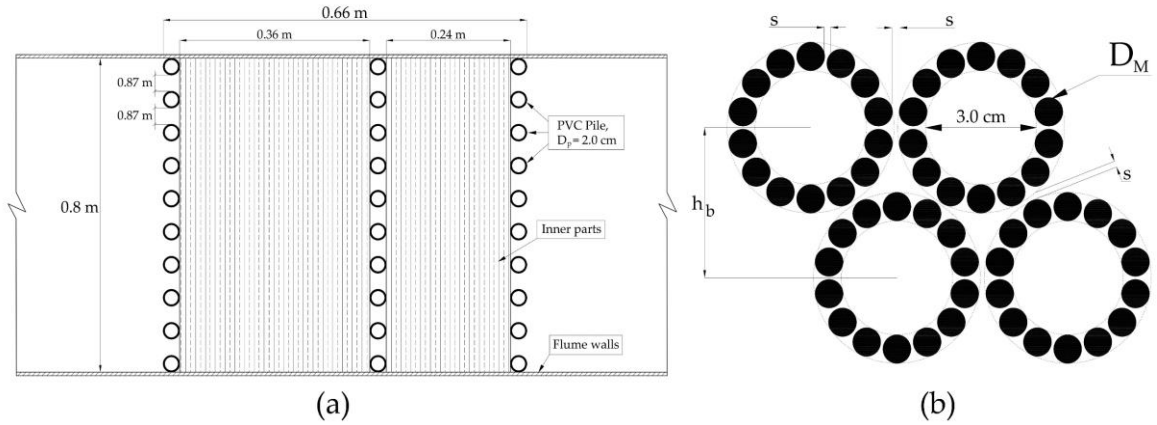

Figure 2. The wooden fence setup. The top-view (a) of the fence and the inner parts (b) structure [9].

2.2. Numerical model

SWASH model is the time-phased averaging model, which can simulate hydrostatic and non-hydrostatic free-surface flow based on the nonlinear shallow water equation [19]. This model can also accurately account for many waves and flow processes on the nearshore [20].

The government equations for wave propagation in a cross-shore profile are:

$$\frac{\partial u}{\partial x}+\frac{\partial w}{\partial z}=0 \quad (1)$$

$$\frac{\partial \eta}{\partial t}+\frac{\partial}{\partial x}\int_{-d}^{\eta} u dz=0 \quad (2)$$

$$\frac{\partial w}{\partial t}+\frac{\partial uw}{\partial x}+\frac{\partial ww}{\partial z}+\frac{1}{\rho}\frac{\partial (P_{nh})}{\partial z}+\frac{\partial \tau_{zz}}{\partial z}+\frac{\partial \tau_{zx}}{\partial x}=0 \quad (3)$$

$$\frac{\partial u}{\partial t}+\frac{\partial uu}{\partial x}+\frac{\partial wu}{\partial z}+\frac{1}{\rho}\frac{\partial (P_h+P_{nh})}{\partial x}+\frac{\partial \tau_{xz}}{\partial z}+\frac{\partial \tau_{xz}}{\partial x}=0 \quad (4)$$

where x is the horizontal coordinate and z is the upward coordinate relative to the still water level. u and w are horizontal and vertical velocities, respectively. η is the free surface elevation relative to the still water level, t is the time. The pressure contribution P is separated into the hydrostatic pressure P_h and nonhydrostatic pressure P_{nh}. The turbulent stresses τ are calculated from a constant turbulent viscosity.

At the bottom boundary, bottom stress is applied, following a quadratic friction law, as:

$$\tau_b=c_f\frac{U|U|}{\eta+d} \quad (5)$$

where U is the depth-averaged velocity; c_f is friction coefficient which is based on Manning's roughness coefficient n [13]:

$$c_f = \frac{n^2 g}{d^{1/3}} \quad (6)$$

The settings of SWASH model are based on the physical model and study [9]. In detail, the 1D-mode was applied with the profile, as shown in Figure 1. A horizontal resolution was set at 0.02 m, and the initial water level was set to zero. The physical condition for SWASH was the vertical turbulence viscosity, which was set as 3×10^{-4} (m^2/s), and the bed friction coefficient, which applied Manning's roughness coefficient as a default factor as 0.019 ($m^{-1/3}s$) [19]. The interpretation for this setup was described in the study [9].

In the SWASH model, two options can be applied to simulate the interaction between waves and wooden fences, the vegetation and porous implementation model. The vegetation model takes into account a number of cylinders in an area and the bulk drag coefficient to calculate the reduction of incoming wave heights as the following equation:

$$\frac{H}{H_0} = \frac{1}{1+\tilde{\beta}x} \quad (7)$$

where H_0 (m) and H (m) are the incoming and transmission wave heights, respectively and the parameter $\tilde{\beta}$ is calculated from [21] yielded as:

$$\tilde{\beta} = \frac{1}{3\sqrt{\pi}}\overline{C_D}DNH_0k\frac{sinh^3(k\alpha H_f) + 3\sinh(k\alpha H_f) + cosh^3(k\alpha H_f) - 3\cosh(k\alpha H_f) + 2}{[\sinh(2kd) + 2kd]\sinh(kd)} \quad (8)$$

where the parameter αH_f is the water depth from the fence's toe to the water surface with H_f is the fence height, k is the wave number and $\overline{C_D}$ is the bulk drag coefficient.

On the other hand, the porous implementation model considers the computational domain to simulate the interaction between waves and porous coastal structures. The mean flow through a porous medium, therefore, is described by the mean volume Reynolds-averaged Navier-Stokes equations. The flow conditions, including laminar and turbulent flow, then is modelled as the respective frictional forces inside the porous medium by the empirical formula of Van Gent [18]:

$$F_D = a\rho u + b\rho|u|u \quad (9)$$

where a (s/m) and b (s^2/m^2) are the friction factors representing viscosity and turbulence dominance, ρ (kg/m^3) is water density, and u (m/s) is the flow velocity. These factors depend on the porosity (n), cylinder diameter (D) and viscosity of water (v), indicated as:

$$a = \alpha\frac{(1-n)^2}{n^3}\frac{\nu}{gD^2} \quad (10)$$

$$b = \beta\frac{1-n}{n^3}\frac{1}{gD} \quad (11)$$

where g (m/s^2) is gravitational acceleration, the set-parameter α and β are the dimensionless parameter representing friction terms.

Moreover, the study [10] stated that the importance of α was always minor and much less than the β in turbulent conditions. Therefore, that study found the relationship between the bulk drag coefficient ($\overline{C_D}$) and the β in turbulent flow conditions as yielded as:

$$\beta = \frac{2n}{\pi}\overline{C_D} \quad (12)$$

This relationship then allows comparing the interaction between wave and fence in different methods, the porous and vegetation models. The details can be found in the study [9].

2.3. Validation

The validation was given a good agreement between the physical and numerical vegetation model, which uses the bulk drag coefficient as shown in Figure 3a [9]. In this study, the validation continues by using the β values calculated directly from $\overline{C_D}$ in Equation 12. In Figures 3a and 3b, the comparison of $\overline{C_D}$ and β in the same relationship with KC number, with $KC = uT_p/D$ where u is flow velocity in front of the fence, T_P is peak wave periods.

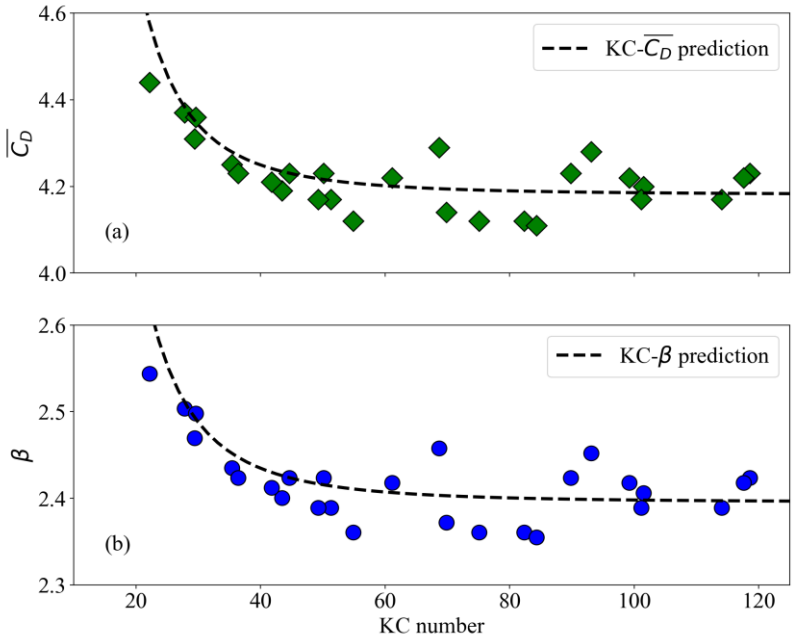

Figure 3. Relationship of the bulk drag coefficient ($\overline{C_D}$) and KC number (a); And the dimensionless coefficient (β) and KC number (b).

Furthermore, the errors between physical and numerical data that is the predictive skill of SWASH are calculated with two parameters, such as bias and scatter index, defined as:

$$bias = \frac{1}{N}\sum_{i=1}^{N}(\varepsilon_{compute}^{i} - \varepsilon_{measure}^{i}) \quad (13)$$

$$SI = \frac{\sqrt{\frac{1}{N}\sum_{i=1}^{N}(\varepsilon_{compute}^{i} - \varepsilon_{measure}^{i})^2}}{\frac{1}{N}\sum_{i=1}^{N}\varepsilon_{measure}^{i}} \quad (14)$$

where $\varepsilon_{compute}$ and $\varepsilon_{measure}$ are the statistical wave values simulated by SWASH and measured in the wave flume, respectively, and N is the total number of data points in the considered data set [22].

3. Results and Discussion

3.1. Wave heights

Figure 4 shows the standing waves of four cases for all models, such as physical (red diamonds), vegetation (solid black line) and porosity (blue dashed line) models. As can be seen, SWASH gives a good simulation which shows the reflection in front and transmission behind the fences for both vegetation and porous models. Moreover, standing waves are compared to each other in Figure 4, showing that the two implementation models agree well with measurement data.

3.2. Surface elevation and Wave spectrum

Figure 5 indicates the water elevation at three locations, x = 19.2 m, 25.3 m (in front of the fence) and x = 30.0 m (behind the fence), of three models, physical model (dashed black line), vegetation model (solid green line), and porous model (solid blue line). The results show a good agreement between the three models even though several phases are delayed between numerical and physical models.

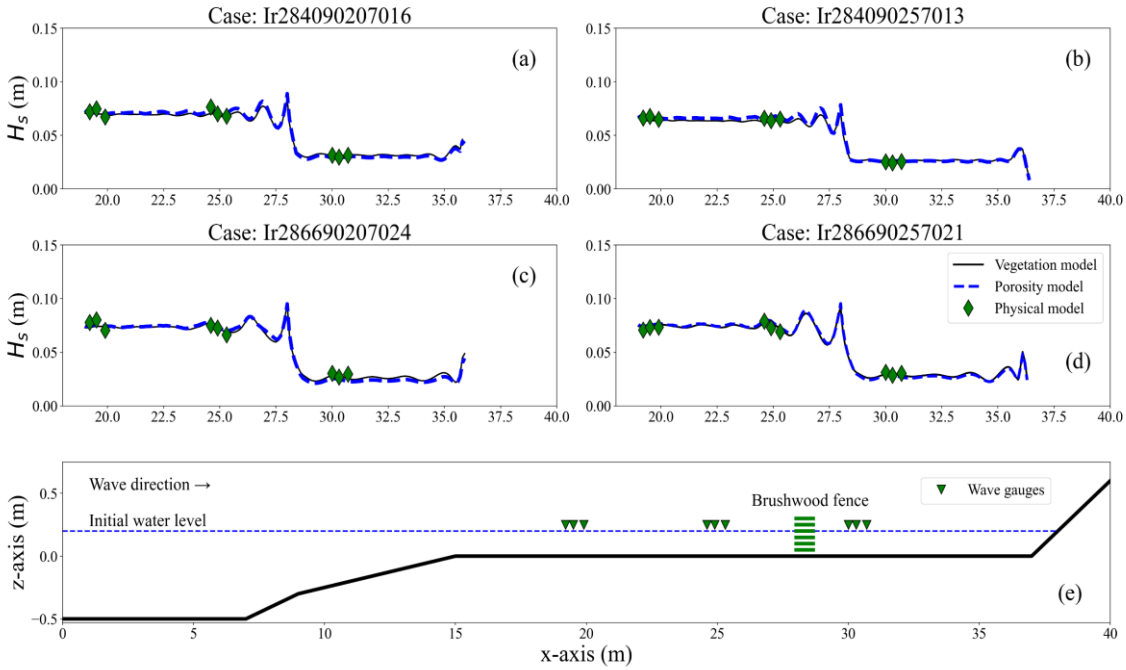

Figure 4. Standing wave heights in four cases: (a) $d = 0.2$ m, $H_s = 0.07$ m, $T_P = 1.6$ s, $B = 0.4$ m; (b) $d = 0.25$ m, $H_s = 0.07$ m, $T_P = 1.3$ s, $B = 0.4$ m; (c) $d = 0.2$ m, $H_s = 0.07$ m, $T_P = 2.4$ s, $B = 0.66$ m; and (d) $d = 0.25$ m, $H_s = 0.07$ m, $T_P = 2.1$ s, $B = 0.66$ m. The profile and measured points are presented in (e).

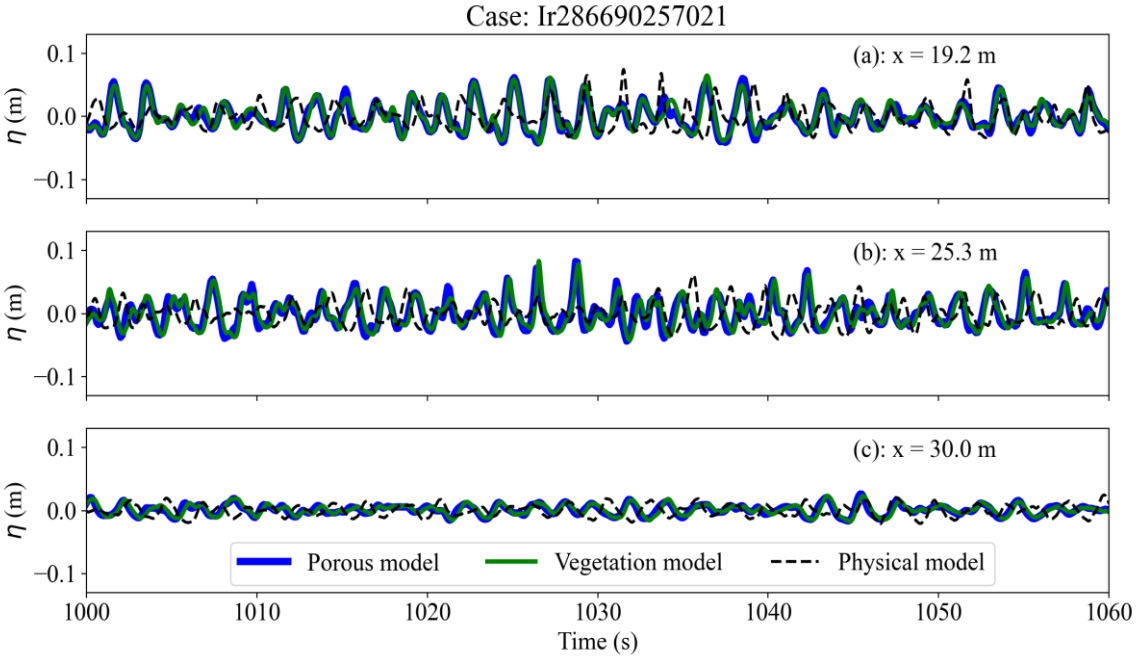

Figure 5. Surface elevation at three locations, in front of the fence x = 19.2 m (a) and x = 25.3 m (b) and behind the fence x = 30.0 m (c).

Figure 5c also indicates the phases lagged due to porous media/vegetation obstruction. It can be seen that water elevation generated from both porous and vegetation models are quite comparable but have less agreement between them and the physical model. This is due to the physical mechanism of wave reduction inside the wooden fence of the physical model might have more inflow between cylinders and larger drag force than described in the SWASH model.

Wave spectra densities of all cases were derived by applying the Fast Fourier Transform (FFT) method to the surface elevation (Figure 5). The wave spectrum of a case at a total of nine wave gauges (Figure 4e) is indicated in Figure 6. As can be seen, all wave spectral densities of all models have a good agreement. There are different densities at frequency of 0.5 for location x = 19.5, 19.9, and 24.9 m. The reflection could cause these differences due to different mechanisms in front of the fence between the three models. Even though the highest spectral densities at x = 24.6, 24.9, and 25.3 m are slightly similar at a frequency of 0.5, the second densities at a frequency of 0.85 show a difference.

Furthermore, in the physical model, the second peak generally represents the second wave interacting with the first wave. In other words, the first wave is slower than the second one, which is shorter, leading to the second peak of spectral densities. The more wave-wave interactions, the more peaks appear. In SWASH, this phenomenon is somehow absurd and challenging to understand.

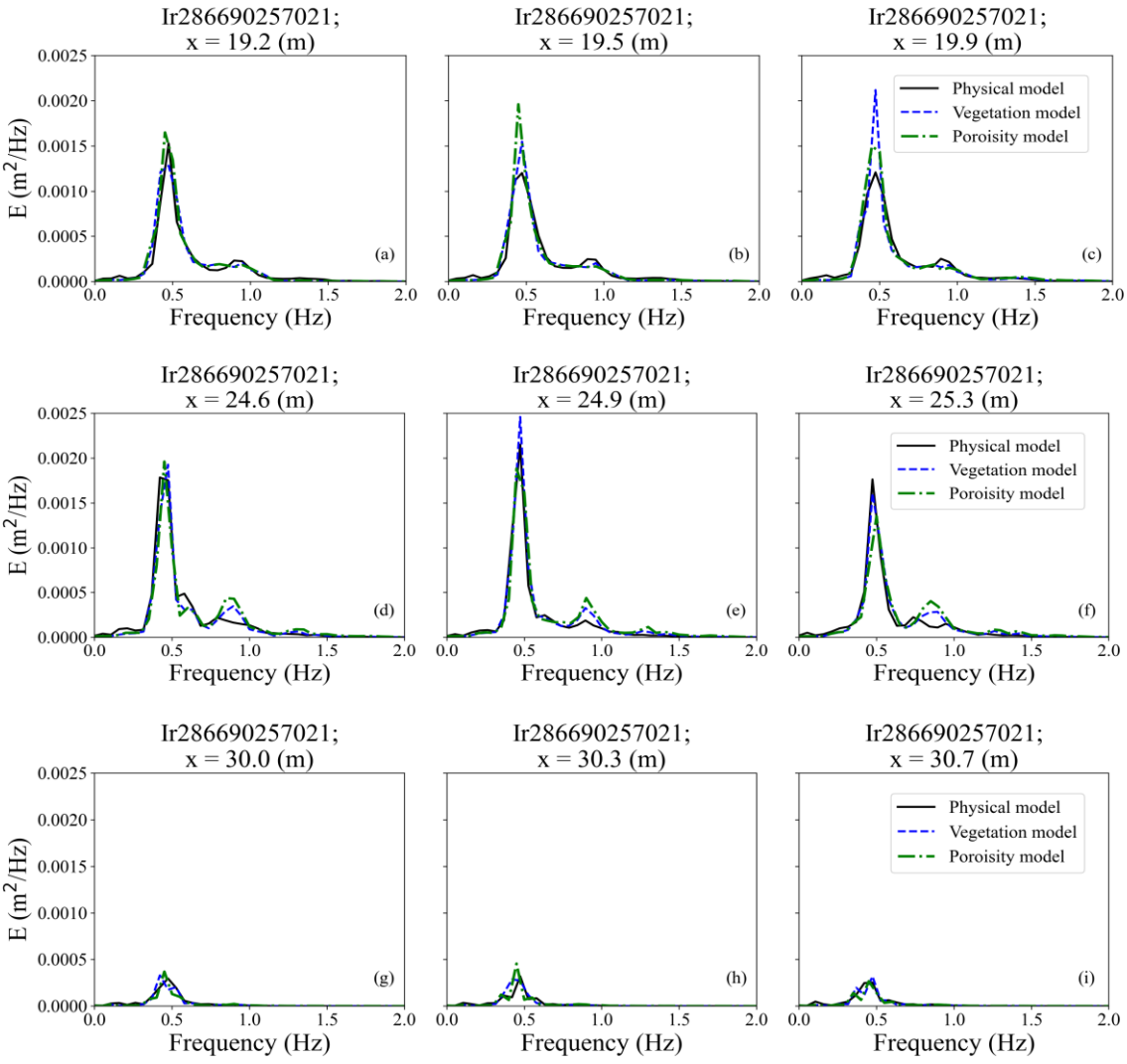

Figure 6. Wave spectrum at nine locations from (a) to (i) of the case: H = 0.07 m, Tp = 2.1s, d = 0.25 m and B = 0.66 m.

3.3. Wave height errors

The skill of SWASH is calculated from Equations 13 and 14 and shown in Figure 7 and Figure 8 for incoming wave heights (in front of the fence) and transmitted wave heights (behind the fence), respectively. The bias and SI parameter gives a good agreement between implementation models (vegetation and porous models) and the physical model. Moreover, for incoming wave heights, the errors are below 5% (Figure 7).

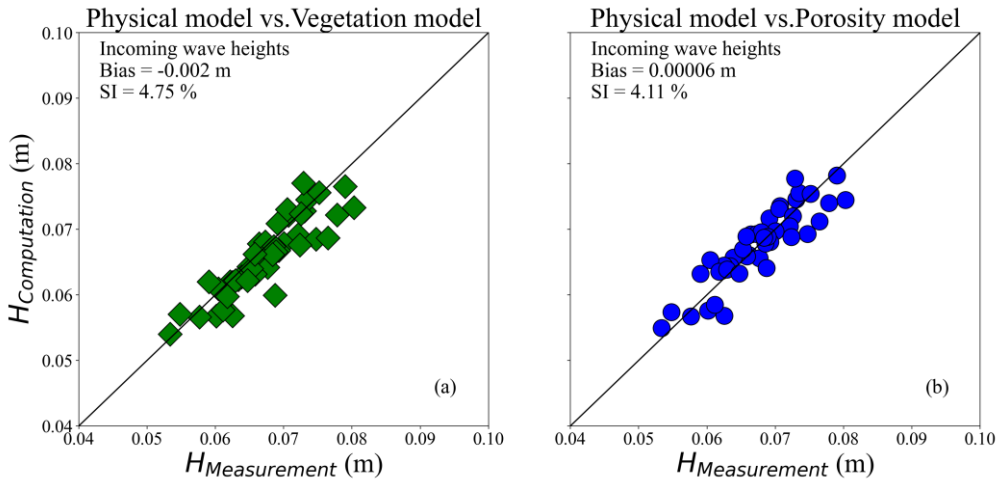

Figure 7. Errors between measurement and numerical data of incoming wave heights for vegetation (a) and porosity (b) implementation model.

However, the transmission wave heights error of the vegetation model is significantly lower than the porous model (Figure 8a). It is shown that the SI value of the vegetation model is about 6%, while this value is nearly double at about 11% for the porous model (Figure 8b). This result means that the skill of SWASH for transmission wave heights for both models is acceptable, but the vegetation model is more accurate than the porous model.

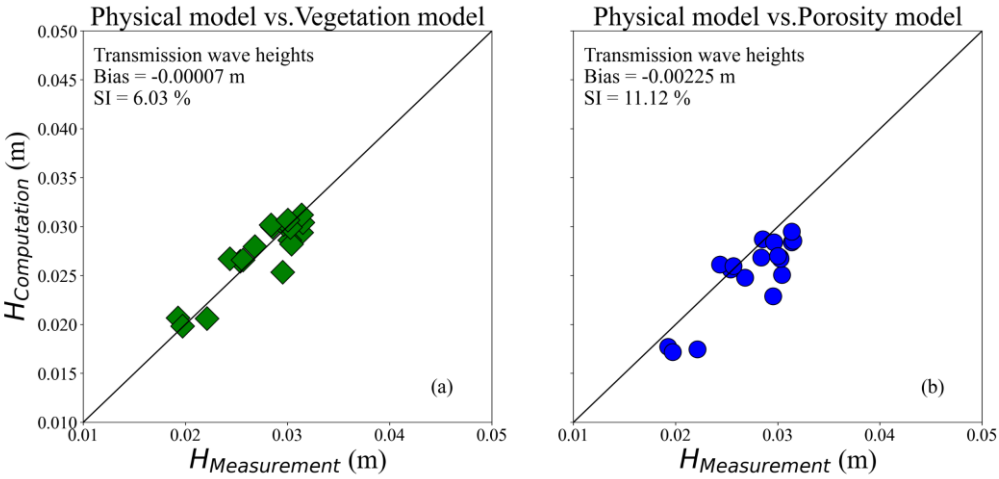

Figure 8. Errors between measurement and numerical data of transmission wave heights for vegetation (a) and porosity (b) implementation models.

4. Conclusion

This study presents an alternative method for validating wave-fence interaction in the SWASH model, the porous implementation model. This model applied the dimensionless friction coefficient (α, β) in the famous Darcy-Forchheimer equations for particularly wooden fences used in the study [9]. Furthermore, the β coefficient has a strong link with the

bulk drag coefficients found in the study [10], which is only effective in the turbulent flow condition.

The validation results of the porous model show a good agreement with the physical and vegetation model for standing wave heights, surface elevations, and wave spectral densities. Moreover, good bias and SI indicate the skill of SWASH even though the errors of the vegetation model are slightly better than the porous model. This study also opens new windows to simulate wave-fence interaction, and more topics, such as sediment transport, and 3D simulation of wave-fence, will be studied in the future.

Author contribution statement: Conceived and designed the experiments; Analyzed and interpreted the data; contributed reagents, materials, analysis tools or data; manuscript editing: H.T.D.; Performed the experiments; contributed reagents, materials, analyzed and interpreted the data, wrote the draft manuscript: H.T.D.; Reviewer and edit: T.M., T.C., T.M.T.D.

Acknowledgement: The first author (Hoang Tung Dao) is grateful for being supported by Delft University of Technology, the Netherlands; Hanoi University of Natural Resources and Environment, Hanoi, Vietnam.

References

1. Schoonees, T.; Mancheño, A.G.; Scheres, B.; Bouma, T.J.; Silva, R.; Schlurmann, T.; Schüttrumpf, H. Hard structures for coastal protection, towards greener designs. *Estuaries Coasts* **2019**, *42(7)*, 1709–1729.
2. Duke, N.; Wilson, N.; Mackenzie, J.; Nguyen, H.H.; Puller, D. Assessment of Mangrove Forests, shoreline condition and feasibility for REDD in Kien Giang Province, Vietnam, Deutsche Gesellschaft für Technische Zusammenarbeit (GTZ), 2010, pp. 1–128.
3. Schmitt, K.; Albers, T. Area coastal protection and the use of bamboo breakwaters in the Mekong Delta. *Coastal Disasters Clim. Change Vietnam, Elsevier* **2014**, 107–132.
4. Albers, T.; San, D.C.; Schmitt, K. Shoreline Management Guidelines: Coastal Protection in the Lower Mekong Delta, GIZ. Eschborn, Germany, 2013.
5. Van Cuong, C.; Brown, S.; To, H.H.; Hockings, M. Using Melaleuca fences as soft coastal engineering for mangrove restoration in Kien Giang, Vietnam. *Ecol. Eng.* **2015**, *81*, 256–265.
6. Van, C.M.; Ngo, A.; Mai, T.; Dao, H.T. Bamboo Fences as a Nature-Based Measure for Coastal Wetland Protection in Vietnam. *Front Mar. Sci.* **2021**, *8*, 1430.
7. Dao, T.; Stive, M.J.F.; Hofland, B.; Mai, T. Wave Damping due to Wooden Fences along Mangrove Coasts. *J. Coastal Res.* **2018**, *34(6)*, 1317–1327. doi: 10.2112/JCOASTRES-D-18-00015.1.
8. Tri, M.C.; Vuong, N.V.; Dat, H.D.; Anh, N.T.T.; Tung, D.H. Numerical simulation of wave transmitting through a bamboo fence. *J. Sci. Technol. Civil Eng.* **2019**, *13(1V)*, 75–83. (In Vietnamese)
9. Dao, H.T.; Hofland, B.; Suzuki, T.; Stive, M.J.F.; Mai, T.; Tuan, L.X. Numerical and small-scale physical modelling of wave transmission by wooden fences. *J. Coastal Hydraul. Struct.* **2021**, *1(4)*, 1–21.
10. Dao, H.T.; Hofland, B.; Stive, M.J.F.; Mai, T. Experimental assessment of the flow resistance of coastal wooden fences. *Water* **2020**, *12(7)*, 1910.
11. Williamson, C.H.K. The natural and forced formation of spot-like "vortex dislocations" in the transition of a wake. *J. Fluid Mech.* **1992**, *243*, 393–441.
12. Schewe, G. On the force fluctuations acting on a circular cylinder in crossflow from subcritical up to transcritical Reynolds numbers. *J. Fluid Mech.* **1983**, *133*, 265–285.

13. Lou, S.; Chen, M.; Ma, G.; Liu, S.; Zhong, G. Laboratory study of the effect of vertically varying vegetation density on waves, currents and wave-current interactions. *Appl. Ocean Res.* **2018**, *79*, 74–87.
14. Zdravkovich, M.M. Flow induced oscillations of two interfering circular cylinders, *J. Sound Vib.* **1985**, *101(4)*, 511–521.
15. Darcy, H.P.G. Les Fontaines publiques de la ville de Dijon. Exposition et application des principes à suivre et des formules à employer dans les questions de distribution d'eau, etc. V. Dalamont, 1856.
16. Forchheimer, P. Wasserbewegung durch boden. *Z. Ver. Deutsch Ing.* **1901**, *45*, 1782–1788.
17. Ergun, S. Fluid flow through packed columns. *Chem. Eng. Prog.* **1952**, *48*, 89–94.
18. van Gent, M.R.A. Wave interaction with permeable coastal structures. *Int. J. Rock Mech. Min. Sci. Geomech.* **1996**, *6(33)*, 277A.
19. Zijlema, M.; Stelling, G.; Smit, P. SWASH: An operational public domain code for simulating wave fields and rapidly varied flows in coastal waters. *Coastal Eng.* **2011**, *58(10)*, 992–1012.
20. Smit, P.; Zijlema, M.; Stelling, G. Depth-induced wave breaking in a non-hydrostatic, nearshore wave model. *Coastal Eng.* **2013**, *76*, 1–16.
21. Suzuki, T.; Hu, Z.; Kumada, K.; Phan, L.K.; Zijlema, M. Non-hydrostatic modeling of drag, inertia and porous effects in wave propagation over dense vegetation fields. *Coastal Eng.* **2019**, *149*, 49–64.
22. Zijlema, M. Modelling wave transformation across a fringing reef using SWASH. *Coastal Eng. Proc.* **2012**, *33*, 1–12.